Colloids and Surfaces B: Biointerfaces 159 (2017) 849–860

Contents lists available at ScienceDirect

Colloids and Surfaces B: Biointerfaces

journal homepage: www.elsevier.com/locate/colsurfb

Research article

Structural analysis of the interaction between Jaburetox, an intrinsically disordered protein, and membrane models

Valquiria Broll[a,1], Anne Helene S. Martinelli[b,1], Fernanda C. Lopes[a], Leonardo L. Fruttero[a,c], Barbara Zambelli[d], Edoardo Salladini[d], Olena Dobrovolska[d], Stefano Ciurli[d,*], Celia R. Carlini[a,c,**]

[a] Graduate Program in Cellular and Molecular Biology – Center of Biotechnology, Federal University of Rio Grande do Sul (UFRGS), Porto Alegre, RS, CEP 91501-970, Brazil
[b] Department of Biophysics, Biosciences Institute (IB), UFRGS, Porto Alegre, RS, CEP 91501-970, Brazil
[c] Brain Institute – BRAINS – InsCer, Pontifícia Universidade Católica do Rio Grande do Sul (PUCRS), Av. Ipiranga 6690, CEP 90610-000 Porto Alegre, RS, Brazil
[d] Laboratory of Bioinorganic Chemistry, Department of Pharmacy and Biotechnology, University of Bologna, Via Giuseppe Fanin 40, I-40127 Bologna, Italy

ARTICLE INFO

Article history:
Received 8 May 2017
Received in revised form 24 August 2017
Accepted 27 August 2017
Available online 30 August 2017

Keywords:
Jaburetox
Model membranes
Intrinsically disordered proteins
Nuclear magnetic resonance
Circular dichroism
Fluorescence microscopy

ABSTRACT

Jack bean urease is entomotoxic to insects with cathepsin-like digestive enzymes, and its toxicity is mainly caused by a polypeptide called Jaburetox (Jbtx), released by cathepsin-dependent hydrolysis of the enzyme. Jbtx is intrinsically disordered in aqueous solution, as shown by CD and NMR. Jbtx is able to alter the permeability of membranes, hinting to a role of Jbtx-membrane interaction as the basis for its toxicity. The present study addresses the structural aspects of this interaction by investigating the behaviour of Jbtx when in contact with membrane models, using nuclear magnetic resonance and circular dichroism spectroscopies in the absence or presence of micelles, large unilamellar vesicles, and bicelles. Fluorescence microscopy was also used to detect protein-insect membrane interaction. Significant differences were observed depending on the type of membrane model used. The interaction with negatively charged SDS micelles increases the secondary and tertiary structure content of the polypeptide, while, in the case of large unilamellar vesicles and bicelles, conformational changes were observed at the terminal regions, with no significant acquisition of secondary structure motifs. These results were interpreted as suggesting that the Jbtx-lipids interaction anchors the polypeptide to the cellular membrane through the terminal portions of the polypeptide and that, following this interaction, Jbtx undergoes conformational changes to achieve a more ordered structure that could facilitate its interaction with membrane-bound proteins. Consistently with this hypothesis, the presence of these membrane models decreases the ability of Jbtx to bind cellular membranes of insect nerve cord. The collected evidence from these studies implies that the biological activity of Jbtx is due to protein-phospholipid interactions.

1. Introduction

Jaburetox (Jbtx) is an intrinsically disordered polypeptide (IDP) released from Jack bean (*Canavalia ensiformis*) urease (JBU) upon hydrolysis performed by cathepsin-like enzymes present in the digestive system of some insects [1–5]. Both JBU and Jbtx feature potential as insecticides, but the activity of the polypeptide is greater than that of urease and it is effective over a broader spectrum of insect orders, because it does not require prior hydrolysis to be active [6,7].

In 2009, Stanisçuaski and co-workers proposed a model in which Jbtx exerts its entomotoxic role by interacting with receptors at *Rhodnius prolixus* Malpighi tubule's membranes, thus altering the eicosanoid signaling pathway, increasing cGMP levels, and disturbing trans-membrane potential, with consequent diuresis inhibition in this insect model [8]. Recently, the central nervous system of *Triatoma infestans* was demonstrated to be a Jbtx target, with the polypeptide interfering in enzymatic pathways of neuronal tissue, both in vivo and in vitro [9]. Later, Fruttero et al. reported that Jbtx

* Corresponding author at: Laboratory of Bioinorganic Chemistry, Department of Pharmacy and Biotechnology, University of Bologna (UniBO), Via Giuseppe Fanin 40, 40127 Bologna, Italy.
** Corresponding author at: Brain Institute – Pontifícia Universidade Católica do Rio Grande do Sul (PUCRS), Av. Ipiranga 6690, 90619-900 Porto Alegre, RS, Brazil.
E-mail addresses: stefano.ciurli@unibo.it (S. Ciurli), celia.carlini@pucrs.br (C.R. Carlini).
[1] The authors VB and AHSM contributed equally to this work.

http://dx.doi.org/10.1016/j.colsurfb.2017.08.053
0927-7765/

affects the defence mechanisms in *R. prolixus* by affecting both the cellular and the humoral immune responses [10]. In addition to insects, the activity of Jbtx against yeasts and filamentous fungi has also been reported, with its fungicidal mechanism of action involving alteration of ions transport, changes in morphogenesis and permeabilization of fungal cells [11].

The biological activities of Jbtx appear to correlate with its ability to interact with cellular membranes, specifically through a protein-lipid interaction that causes the alteration of membrane structures with the possible formation of pores [12–15]. In 2009, Barros and co-workers showed that incubation with Jbtx leads to disruption of large unilamellar vesicles (LUVs) and release of a pre-loaded fluorescent dye [12]. Additionally, Martinelli and co-workers [15] reported that both the N- and the C-terminal half portions of Jbtx were able to interact with lipid vesicles and disrupt them in a similar way as observed for the entire polypeptide.

Recently, the secondary and tertiary structures of Jbtx were established using circular dichroism (CD) and nuclear magnetic resonance (NMR) spectroscopies [5]. The CD spectrum is typical of an intrinsically disordered protein, a result confirmed by NMR, which further revealed the presence of regions with transient secondary structure, such as a short α-helical motif in the N-terminal region and two turn-like structures, one located in the central region and another near the C-terminal of the polypeptide [5].

Intrinsically disordered proteins (IDPs) are described as molecules with a wide range of folding possibilities. Typically, IDPs are composed of *foldons*, portions of a protein that can be folded independently, and *unfoldons*, regions of the protein that dynamically move from order-to-disorder to be biologically functional [16,17]. This behaviour is classified as (i) *binding-induced folding*, when the disorder-to-order path is absolutely needed to achieve the biological function, (ii) *binding-induced transient folding,* when IDPs are critically involved in signalling interactions, participating in on-off type systems, (iii) *binding-induced folding divergence,* characteristic of proteins with the ability to bind to different partners, (iv) *binding-induced under-folding,* applied to a system in which the connection to the partner generates a partial fold in the IDP, and as (v) *binding and non-folding,* when the interaction is dependent on the flexibility of the protein [17,18].

Many IDPs are known to interact with cellular membranes [19], whether natural or artificial. To mimic cellular membranes, ionic surfactants have been largely and successfully used in the determination of protein structure, mainly for proteins that are unstructured, such as IDPs [20]. Sodium dodecyl sulphate (SDS), when in concentrations above its critical micelle concentration (CMC), can be used as a mimetic membrane due to its ability to influence protein secondary structure similarly to what is observed for natural membranes [20,21].

Due to the remarkable resemblance of lipid bilayers to natural membranes, artificial lipid vesicles have been used as mimetic cellular membranes to provide structural and quantitative information regarding protein-membrane interactions [21,22]. In the past twenty years, bicelles have also emerged as a new class of membrane model for solid-state NMR that provides structural information of hydrophobic molecules in their native state [23,24]. Bicelles are composed of a mixture of phospholipids and detergent. The most used combination is the lipid dimyristoyl-phosphatidylcholine (DMPC) with the detergent dihexanoyl-phosphatidylcholine (DHPC), which can be manipulated in order to control the size and its ability to orientate itself in a magnetic field by controlling the lipid/detergent concentration rate (q-ratio) [23,25]. Small bicelles have been used to evaluate protein structure as well as protein-membrane interaction [20,26].

In this work, we investigated the interaction of the intrinsically disordered Jbtx polypeptide with detergents and lipids (micelles, large unilamellar vesicles and bicelles) at the molecular level, by using CD and NMR spectroscopy, as well as fluorescence microscopy.

2. Materials and methods

2.1. Cell culture and protein purification

The construct containing the Jbtx with a C-terminal His-tag sequence was introduced into a pET-23a vector as described in Postal et al. [11], and the corresponding protein sequence is composed of 100 amino acids (MGPVNEANCK-AAMEIVCRREFGHKEEEDASEGVTTGDPDCPFTKAIPREEYANKYG-PTIGDKIRLGDTDLIAEIEKDFALYGDESVFGGGKVISHHHHHH), as reported in Lopes et al. [5]. This vector was used to transform *Escherichia coli* BL21(DE3) (Novagen, Madison, WI, USA) by heat shock. The expression was performed using a previously described protocol [5]. ^{15}N labelled protein expression was performed by addition of $(^{15}NH_4)_2SO_4$ in M9 medium (Sigma-Aldrich, St. Louis, MO, USA). The purification followed the previously reported protocol [5] with some modifications. In detail, the cellular pellet was harvested by centrifugation (11,000*g* for 10 min at 4 °C) and resuspended in 30 mL of buffer A (50 mM Tris-HCl, pH 7.5, 500 mM NaCl, 20 mM Imidazole). Cells were disrupted by three passages of the crude extract through a French pressure cell system (SLM, Aminco, Haverhill, MA, USA) at 20,000 psi. Following the removal of cell debris by centrifugation at 27,200*g* for 40 min at 4 °C, the supernatant was applied onto a Ni(II)-loaded 5 mL His-Trap HP column (GE Healthcare, Little Chalfont, UK) previously equilibrated in buffer A. The affinity resin was washed with 20 column volumes (CV) of buffer A. After this step, the imidazole concentration was increased up to 70 mM in order to remove weakly bound contaminants. The affinity column was then connected in tandem to a Superdex 75 16/60 column (GE Healthcare, Little Chalfont, UK) pre-equilibrated in 50 mM sodium phosphate buffer (NaPB) at pH 7.5, containing 1 mM EDTA and 1 mM TCEP. The two connected columns were eluted, first using 25 mL of buffer A containing 500 mM imidazole, and subsequently using 50 mM sodium phosphate buffer (NaPB) at pH 7.5, containing 1 mM EDTA and 1 mM TCEP (Fig. S1A). The fractions containing Jbtx were collected, concentrated using 3 kDa Amicon Ultra Centrifugal Filters (Merk Milllipore, Darmstadt, Germany) and loaded onto a Superdex 75 10/300 column (GE Healthcare, Little Chalfont, UK), equilibrated with the same buffer at pH 6.5 (Fig. S1B); the final fractions were concentrated as above and stored at −80 °C.

Fractions of all purification steps were analyzed by SDS-PAGE using NuPAGE Novex 12% Bis-Tris gels (Life technologies, Carlsbad, CA, USA) and staining with ProBlue Safe Stain (Giotto Biotech, Sesto Fiorentino, Italy). Protein quantification was performed by the Bradford assay [27] and by absorbance at 280 nm considering a molar extinction coefficient of 4595 M^{-1} cm^{-1} [28]. The final yield was ca. 30 mg of pure protein per liter of culture.

2.2. Preparation of model membranes

2.2.1. SDS micelles

SDS micelles were prepared starting from 300 mM SDS (Sigma Aldrich, St. Louis, MO, USA) stock solutions. The critical micelle concentration (CMC) of SDS in 50 mM NaPB pH 6.5, 1 mM EDTA, 1 mM TCEP and in MilliQ water (control) were estimated by measuring the conductivity at controlled temperature, as previously described [29].

2.2.2. Large Unilamellar Vesicles (LUVs)

Large unilamellar vesicles (LUVs) were prepared by the extrusion method [30,31], using lipids (*10* mg/mL in *chloroform*) purchased from Avanti Polar Lipids Inc. (Alabaster, AL,

USA). Lipid chloroform solutions were prepared using a mix of lipids in different molar ratios: phosphatidylglycerol (PG, 100%), phosphatidylcholine:phosphatidylglycerol (PC:PG, 50:50%), palmitoyl-oleoyl phosphatidyl cholin (POPC, 100%), palmitoyl-oleoyl phosphatidyl cholin:ergosterol (POPC:Erg, 70:30%) and phosphatidylethanolamine:phosphatidylcholine (PE:PC, 50:50%). A lipid film was formed by drying the chloroform under nitrogen flow, then rehydrated in the appropriate buffer and resuspended by vortexing. The lipid mixture was processed at least 20 times in a mini-extruder (Avanti Polar Lipids Inc., Alabaster, AL, USA) through a polycarbonate filter membrane with pores of 100 nm diameter, at room temperature. The result was a stock suspension of LUVs containing a total of 5 mM phospholipids in 50 mM NaPB at pH 6.5 (for CD spectroscopy) or 45 mM in 50 mM NaPB pH 6.5 containing 1 mM EDTA, 1 mM TCEP and 10% D_2O (for NMR spectroscopy).

2.2.3. Bicelles

The lipids 1,2-dihexanoyl-*sn*-glycero-3-phosphatidylcholine (DHPC), 1,2-dimyristoyl-*sn*-glycero-3-phosphatidylcholine (DMPC), and 1,2-dimyristoyl-*sn*-glycero-3-phosphatidylglycerol (DMPG) were purchased as dry powders from Avanti Polar Lipids Inc. (Alabaster, AL, USA). Bicelle samples were prepared by suspending the appropriate amount of DMPC, DHPC and DMPG in 50 mM NaPB at pH 6.5, to achieve a [DMPC/DHPC] or [(DMPC:DMPG)/DHPC] molar ratio (q) of 0.5, and a total concentration of 250 mM of lipid mix. DHPC and DMPC were combined at 66.6:33.4 molar ratio to prepare neutral bicelles, while a combination of DHPC:DMPC:DMPG at 66.6:16.7:16.7 ratio was used to formulate negatively charged bicelles. The procedure followed a published protocol [32,33] and involved 10 freeze-thaw cycles alternated with vortexing, resulting in a uniform transparent non-viscous emulsion in 50 mM NaBP. For NMR analysis, 1 mM EDTA and 1 mM of TCEP were added.

2.3. Fluorescence microscopy

2.3.1. Fluorescent labeling

Jbtx conjugation with fluorescein isothiocyanate (Jbtx-FITC) was carried out by incubating 50 mM jaburetox and 48 μg/mL of FITC (Sigma-Aldrich, St. Louis, MO, USA) prepared in DMSO at room temperature for 2.5 h [34] in 50 mM NaPB pH 6.5, containing 1 mM EDTA and 1 mM TCEP. The excess of FITC was removed from the sample using a HiTrap desalting 5 mL column (GE Healthcare, Little Chalfont, UK). The same procedure was repeated with bovine serum albumin (BSA), used as a non-specific interaction control (BSA-FITC). The FITC-labelled proteins were used in the interaction assays with cockroach nerve cord and *Saccharomyces cerevisiae*.

2.3.2. Yeast interaction assay

S. cerevisiae was cultured in Sabouraud media overnight at 28 °C with constant agitation. The cell concentration was estimated by optical density (OD_{600}) and adjusted to 0.6. The incubations with Jbtx-FITC and BSA-FITC (23 μM) were performed for 3 h at 4 °C or for 1 h at 28 °C [35]. These preparations were analyzed using the EVOS FLoid cell Imaging Station fluorescence microscope (Thermo Scientific, Waltham, MA, USA) and the Axioskop 40–Zeiss with Axiocam MRc (Carl Zeiss, Jena, Germany) fluorescence microscope, respectively.

Alternatively, yeast cells were lysed after incubation with the labelled proteins (3 h at 28 °C) using glass beads (200 nm) and vortex (four cycles of 1 min and 30 s of ice bath among cycles). The lysed cells were centrifuged at 10,000*g* for 10 min, the supernatant was removed, and the pellet was washed three times with 50 mM NaPB at pH 7.5, containing 1 mM EDTA and 1 mM TCEP. The pellets were observed under UV light (Molecular Imager Gel Doc XR-Bio-Rad, Bio-Rad Laboratories, Hercules, CA, USA).

2.3.3. Nerve Cord (NC) interaction assay

Cockroaches (*Nauphoeta cinerea)* were maintained with free access to food and water, under controlled temperature between 22 and 25 °C and 12:12 h light:dark cycles. Adults were cooled at −20 °C for 5 min and immobilized ventral side up to have their body cavity opened. The nerve cord (NC), composed by pro, meso and metathoracic ganglia, was dissected, and removal of other tissues was done under constant bathing with 20 mM NaPB pH 6.5 containing single-use protease inhibitors cocktail (Thermo Scientific, Waltham, MA, USA). The incubation of Jbtx-FITC and BSA-FITC with the NC was carried out by incubation with 23 μM solutions of either protein for 1 h at room temperature. Three washes were performed with buffer (30 min each) at room temperature. The NC were placed in Lab-Tek Chamber slides (Thermo Scientific, Waltham, MA, USA) and analyzed using an inverted microscope Zeiss Axiovert 200 equipped with an Axiocam MRc (Carl Zeiss, Jena, Germany), with AxioVision Rel 4.8 as image acquisition software. Alternatively, homogenates of NC, after exposition to FITC-labelled proteins and washes, were prepared by using glass beads (200 nm) and vortex (4 cycles of 1 min and 30 s of ice bath among cycles). The lysed tissue was centrifuged at 10,000*g*, during 10 min, the supernatant removed and the pellet washed 3 times with 50 mM NaPB at pH 6.5, containing 1 mM EDTA and 1 mM TCEP. The pellet was observed under UV light (Molecular Imager Gel Doc XR-Bio-Rad, Bio-Rad Laboratories, Hercules, CA, USA).

Fluorescence microscopy with NC and Jbtx-FITC was also performed in the presence of all the artificial membranes described in this work. The fluorescence was measured using a Spectramax M5 Microplate Reader (Molecular Devices, Sunnyvale, CA, USA), with the treated NC placed in 96-wells black plates (Thermo Scientific, Waltham, MA, USA). All fluorescence measurements were expressed as a ratio between fluorescence emission and NC mass (mg).

2.4. Circular Dichroism (CD) spectroscopy

Circular dichroism spectra of 25 μM Jbtx solutions in 50 mM NaPB at pH 6.5 were recorded in 0.1 cm path length cuvettes at 25 °C using a Jasco 810 spectropolarimeter (Jasco Inc., Easton, MD, USA) in the 190 − 260 nm range, as a function of different amounts of SDS micelles, LUVs or lipid bicelles. The fraction of α-helices of the protein was calculated from mean residue ellipticity at 222 nm as previously reported [36,37]. Care was taken to obtain signals below the maximum value of the high-tension (HT) voltage, as provided by the spectropolarimeter manufacturer (700 V).

2.5. Nuclear magnetic resonance (NMR)

Samples of ca. 0.5 mM ^{15}N-labelled Jbtx in 50 mM NaPB at pH 6.5, containing 1 mM EDTA 1 mM TCEP and 10% (v:v) D_2O were used for NMR spectroscopy. Standard ^{1}H,^{15}N-HSQC spectra were acquired on a Bruker Avance 700 Spectrometer (Bruker Corporation, Billerica, MA, USA) as previously reported [5] in the absence and presence of different amounts of SDS micelles, LUVs or lipid bicelles. All data were processed using iNMR v.5.4.5 (www.inmr.net) and standard processing parameters.

3. Results

3.1. Interaction of Jbtx with biological membranes

Fluorescence microscopy demonstrated the occurrence of an interaction between *S. cerevisiae* and Jbtx-FITC (Fig. 1). This interac-

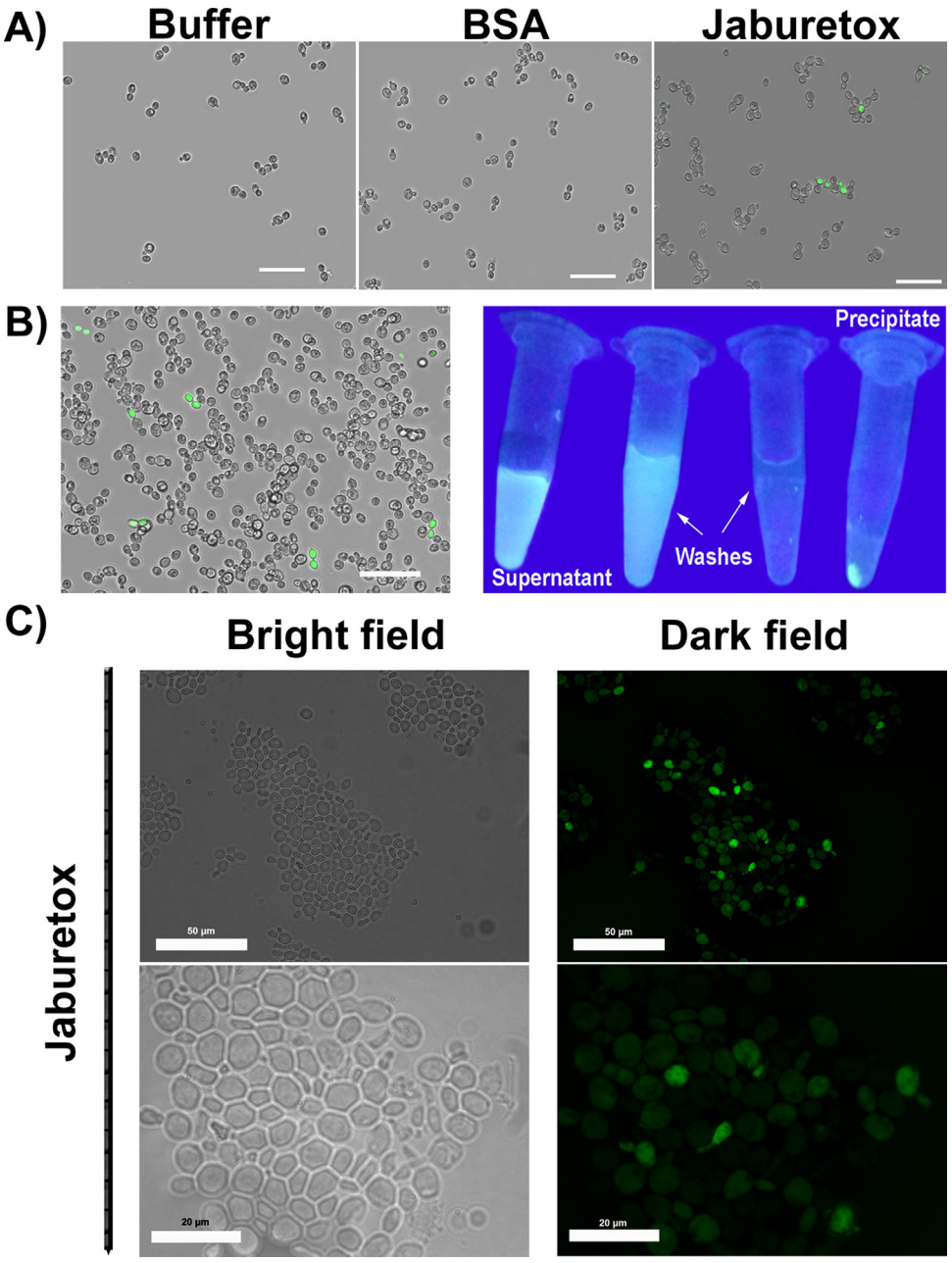

Fig. 1. Interaction of Jbtx-FITC with yeast cells as analyzed by fluorescence microscopy. **A**) *S. cerevisiae* cells after incubation with 23 μM Jbtx-FITC for 3 h at 4 °C (bar: 200 μm; magnification 100 X; the pictures are merged (bright and dark fields)); the left and center panel show the same cells in buffer alone or containing BSA-FITC, while the right panel shows the cells in the presence of Jbtx-FITC. **B**) Left panel: *S. cerevisiae* cells after incubation with 23 μM Jbtx-FITC (3 h at 28 °C), lysed using glass beads; right panel: supernatants and debris of lysed cells visualized under UV light (bar: 200 μm, magnification 200 X); **C**) *S. cerevisiae* cells after incubation with 23 μM Jbtx-FITC for 1 h of at 28 °C; in the top and bottom panels the magnification is 400X (bar = 50 μm) and 1000X (bar = 20 μm), respectively; the left and right panels are distinguished by bright and dark field, respectively. In all cases, the excitation wavelength was 495 nm, and the emission was read at 519 nm.

tion was not observed using BSA-FITC (Fig. 1A), indicating a specific response to Jbtx. Similar experiments also revealed an interaction between the cockroach nerve cord (NC) and Jbtx-FITC, which appeared in greater intensity at the ganglia (Fig. 2). Experiments with a BSA-FITC conjugate performed in the same conditions indicated the absence of an interaction between the FITC moiety and lipids, supporting the specificity of the Jbtx interaction with NC (Fig. 2A). Fluorescence microscopy further proved that Jbtx-FITC interacts with the membrane debris obtained after cellular lysis of *S. cerevisiae* (Fig. 1B) and tissue homogenates of NC (Fig. 2B). In order to investigate the nature of this interaction, competition experiments were designed in which fluorescence microscopy, circular dichroism and NMR spectroscopy were used to monitor the influence of the presence of SDS micelles, LUVs and bicelles on the Jbtx structure and function with respect to biological membranes. In particular, the results of exploratory experiments, shown in Fig. 4, revealed how increasing concentrations of SDS and different kinds of lipids affected the Jbtx-membranes interaction as probed using fluorescence microscopy, prompting more detailed experiments using a multiplicity of spectroscopic approaches aimed at the determination of the secondary and tertiary structure of the polypeptide in the different conditions.

3.2. Interaction of Jbtx with SDS Micelles

The critical micelle concentration (CMC) of SDS was determined by conductivity to be above 1.5 mM in 50 mM NaPB at pH 6.5, containing 1 mM EDTA and 1 mM TCEP (Fig. 3 A). When incubated

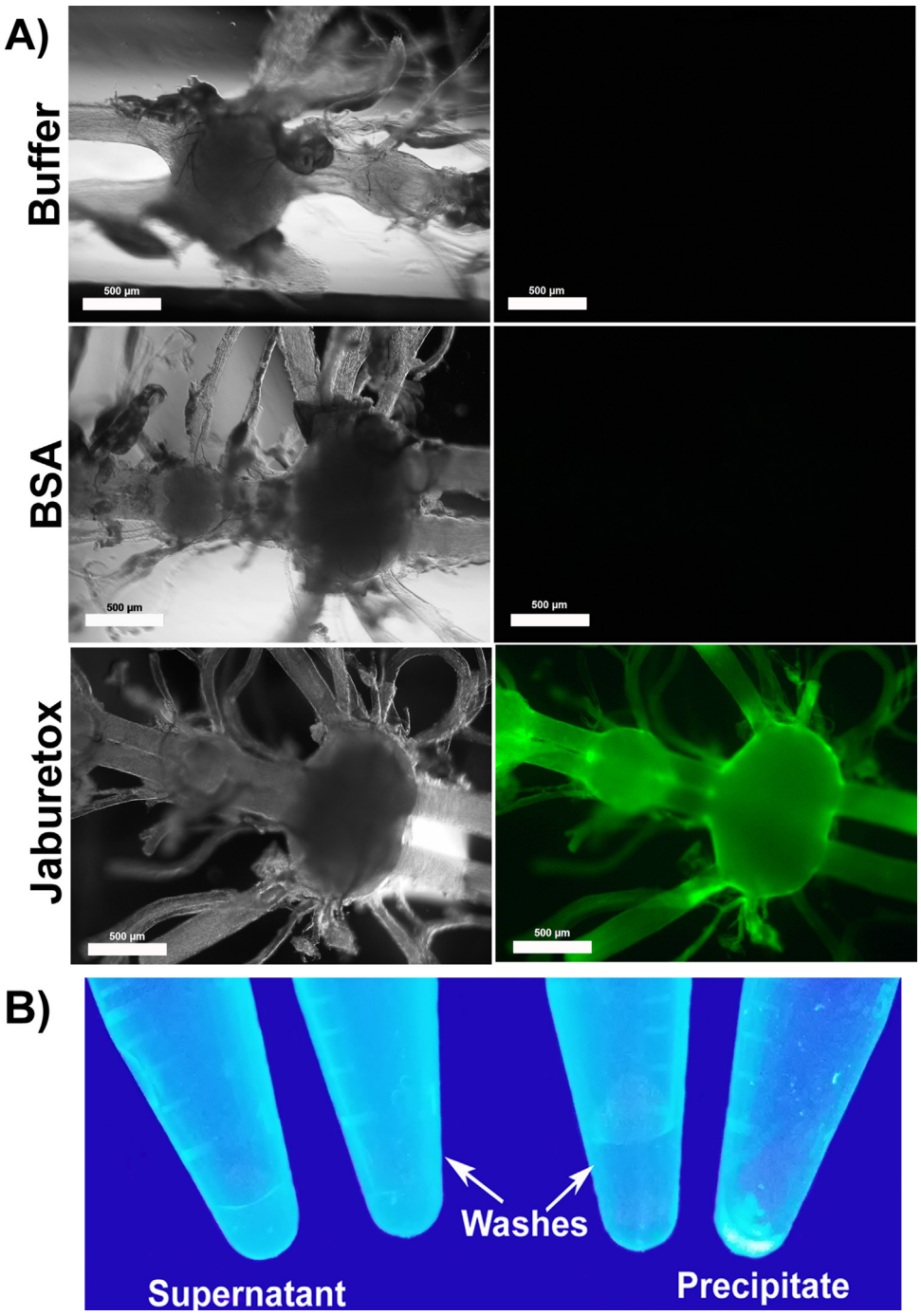

Fig. 2. Interaction of Jbtx-FITC with the nerve cord (NC) of the cockroach *N. cinerea* as analyzed by fluorescence microscopy. **A**) NC after incubation with 23 µM Jbtx-FITC for 1 h at room temperature in bright field (left panels) and dark field (right panels) in the presence of buffer only (top panels), BSA-FITC (middle panels) or Jbtx-FITC (bottom panels). Magnification of 50X, bars: 500 µm; excitation wavelength at 495 nm, emission read at 519 nm. **B**) Homogenates of NC after incubation with Jbtx-FITC after cellular lysis. Supernatant and tissue debris visualized under a UV lamp.

at room temperature and analyzed by CD, the obtained micelles were able to induce modifications of the secondary structure of Jbtx (Fig. 3B). Indeed, while the CD spectrum of Jbtx in the absence of SDS presented a minimum centred at ca. 200 nm, characteristic of a random coil conformation, in the presence of 3–15 mM SDS this feature shifted to ~205–210 nm, with the insurgence of a minimum at around 207 nm, typical of the presence of α-helices and β-sheets; consistently, the ellipticity increase around 195 nm suggests the acquisition of secondary structure by Jbtx in the presence of SDS micelles. A second minimum appeared at 222 nm, indicating the increase in the α-helical content from 5.8% to 13.6%, in the absence and in the presence of SDS, respectively. The $^{1}H,^{15}N$-HSQC NMR spectrum of Jbtx, recorded in the absence and presence of SDS below and above its CMC (0.25 and 10–15 mM, respectively, Fig. 3C) reveals that the protein does not change its structure in the presence of SDS below its CMC, while large chemical shifts modifications are observed in solutions containing SDS above the CMC, indicative of structural conformational changes. Attempts to specifically assign the NMR signals to the amino acid sequence of Jbtx in the presence of SDS above the CMC, using triple resonance experiments and the same approach used for Jbtx in aqueous solution [5] failed due to the lack of key through-bond connectivities, likely

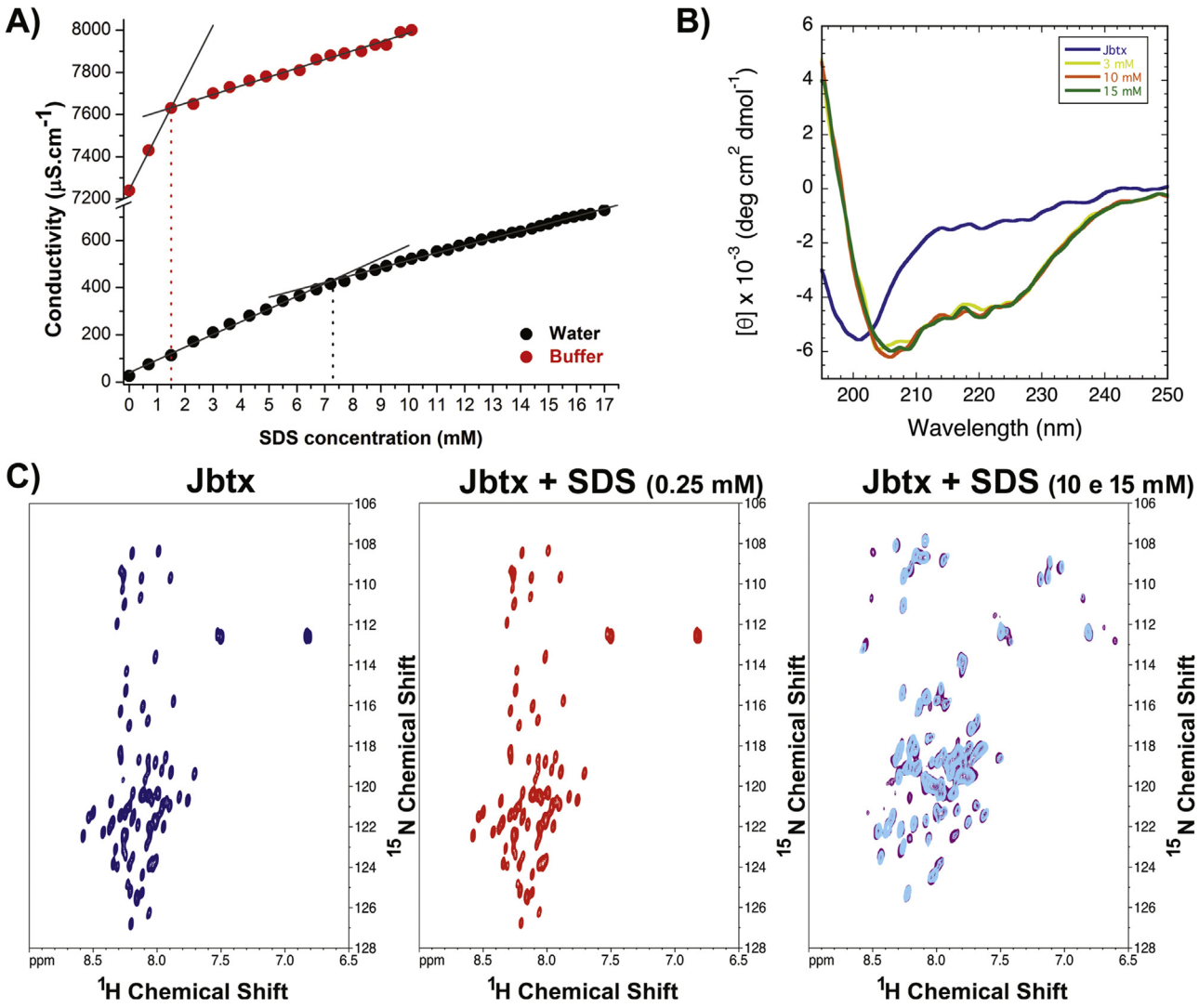

Fig. 3. Structural analysis of Jaburetox in the presence of SDS micelles. **A**) Determination of SDS critical micelle concentration (CMC) by conductivity measurements; red: 50 mM NaPB pH 6.5, 1 mM EDTA, 1 mM TCEP (NaPB, pH 6.5); black: MilliQ water. **B**) Circular dichroism spectra of Jbtx in NaPB at pH 6.5 in the absence and presence of SDS in concentrations above its CMC (yellow: 3 mM SDS; orange: 10 mM SDS; green: 15 mM SDS). **C**) 700 MHz ^{1}H,^{15}N-HSQC spectra of Jbtx (0.5 mM in NaPB pH 6.5) in the absence of SDS (left panel), with 0.25 mM SDS (center panel), and 10 mM or 15 mM SDS (right, violet or light blue). (For interpretation of the references to colour in this figure legend, the reader is referred to the web version of this article.)

reflecting conformational changes in the intermediate time-scale regime. This observation, although qualitative, suggests that Jbtx decreases its mobility upon interaction with SDS micelles.

3.2.1. In vitro *interaction of Jbtx-FITC with insect nerve cord in the presence of SDS micelles*

Fluorescence microscopy experiments were performed to analyse the interaction of the protein with insect nervous tissues in presence of SDS. Jbtx-FITC and insect NC were incubated in the presence of micelles prepared with different concentrations of SDS. The interactions were estimated by fluorescence microscopy as well as by fluorimetry (Fig. 4A). In the presence of SDS below its CMC (0.1 mM), fluorescence intensity of Jbtx-FITC remained comparable to the control (Fig. 4A). On the other hand, a decrease in NC fluorescence was observed upon exposure of Jbtx-FITC to SDS concentrations above the CMC (10 mM). The binding of Jbtx-FITC to cockroach NC was reduced to ca. 25%, when either the labelled protein or the NC were pre-incubated in 10 mM SDS micelles solutions (Fig. 4A). These results indicate that SDS and insect NC compete for Jbtx interaction.

3.3. *Interaction of Jbtx with Large Unilamellar Vesicles (LUVs)*

In order to follow the modifications in the secondary structure of Jbtx, CD spectra were recorded as a function of different amounts of LUVs. No structural changes of Jbtx were detected in the presence of a mixture of PC and PG lipids in a proportion of 50:50 (w/w) (Fig. 5 A) up to a final concentration of 1.0 mM. Negatively charged vesicles, containing only PG (Fig. 5B), produced a slight change in the CD spectrum at lipid concentrations above 1.0 mM. Although the NMR spectrum of Jbtx in the presence of 2 mM PG indicated no significant changes of the tertiary structure, some peaks related to amino acids at the N- and C-termini showed a decrease of intensity under this condition (Fig. 5C), indicative of changes in the peptide dynamics in these regions of the polypeptide.

Jbtx was also tested in the presence of other lipid components, such as PE:PC, POPC or a mixture of POPC and ergosterol in a proportion of 70:30 (w/w) (Fig. 6). In the presence of LUVs composed by PE:PC, a neutral lipid combination, Jbtx did not acquire any secondary structure (Fig. 6A). However, in the presence of POPC, a zwitterionic phospholipid, or POPC:Erg, the CD spectra of Jbtx

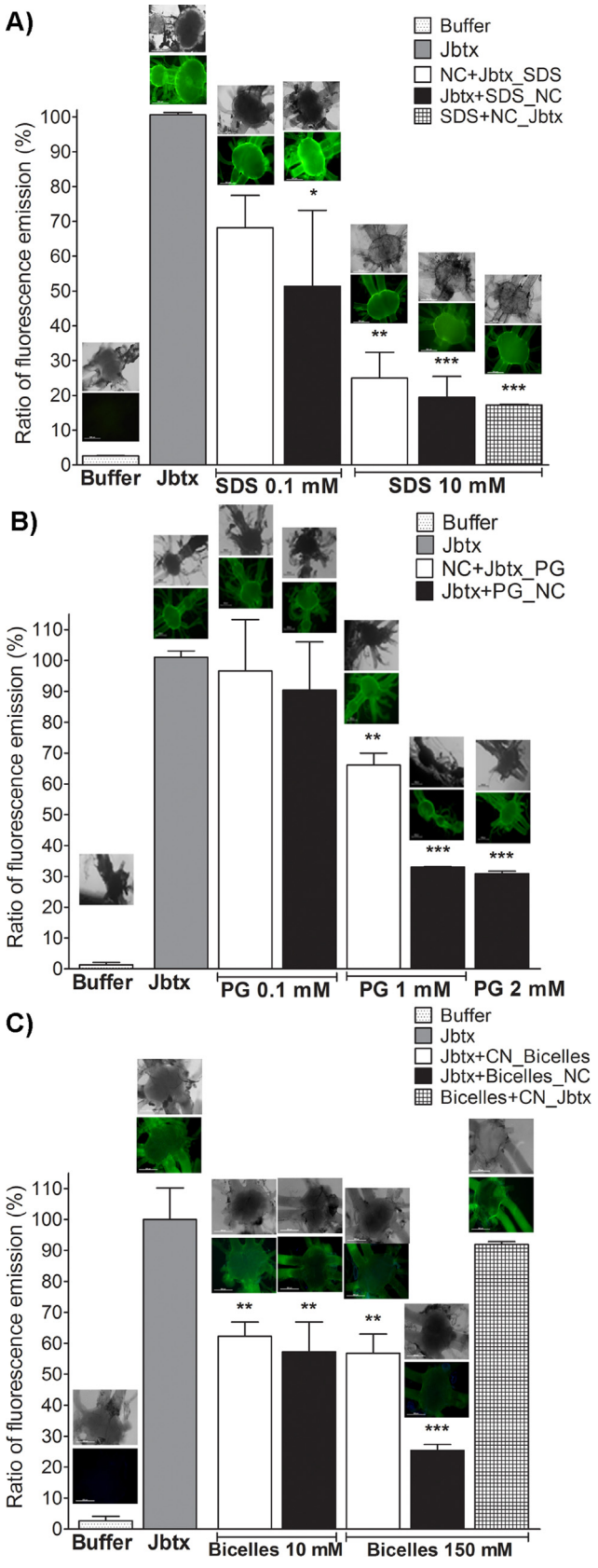

Fig. 4. Interaction of Jbtx-FITC with the nerve cord (NC) of the cockroach *N. cinerea* in the presence of micelles, LUVs and bicelles were analyzed by fluorescence microscopy. **A**) Fluorescence was recorded for NC after incubation with Jbtx-FITC in the absence or presence of 0.1 and 10 mM SDS concentrations. NC incubated with buffer alone (negative control, hatched bar), with Jbtx-FITC (positive control, gray bar), with Jbtx-FITC followed by a vigorous wash with buffer and then added with different concentrations of SDS (white bars), with a solution of Jbtx preincubated with SDS (black bars) or with SDS followed by Jbtx (plaid bar). **B**) Fluorescence was recorded for NC after incubation with Jbtx-FITC in the absence or presence of LUVs made only of PG in different concentrations (0.1, 1.0 and 2.0 mM). NC incubated with buffer alone (negative control), with Jbtx-FITC (positive control, gray bar), with Jbtx-FITC followed by a vigorous wash with buffer and then added with different concentrations of PG LUVs (white bars), with a solution of Jbtx preincubated with PG LUVs (black bars). **C**) Fluorescence was recorded for NC after incubation with Jbtx-FITC in the absence or presence of 10 and 150 mM negatively charged bicelles made by a mixture of DHPC:DMPC:DMPG in a molar ratio of 66.6:16.7:16.7. NC incubated with buffer alone (negative control, hatched bar), with Jbtx-FITC (positive control, gray bar), with Jbtx-FITC followed by a vigorous wash with buffer and then added with different concentrations of bicelles (white bars), with a solution of Jbtx preincubated with bicelles (black bars) or with bicelles followed by Jbtx (plaid bar). The interaction was expressed as the percentage of the ratio of fluorescence emission and NC mass (mg), considering the value obtained for Jbtx-FITC alone as 100%. Data are mean ± S.E.M. (**$p < 0.05$) and performed as a triplicate. In all cases, the concentration ot Jbtx-FITC was 23 μM (magnification 50X).

showed a more pronounced in absence of ergosterol (compare Fig. 6B and C).

3.3.1. In vitro *interaction of Jbtx-FITC with insect nerve cord in the presence of LUVs*

Fluorescence microscopy experiments were performed to analyse the interaction of the protein with insect nervous tissues in presence of LUVs. The results of experiments conducted by incubating Jbtx-FITC and insect NC in the presence of LUVs (Fig. 4B) indicated that negatively charged LUVs (made with PG above 1 mM concentration) affected the interaction. In particular, preincubation of Jaburetox with 1 mM PG-based LUVs decreased the subsequent binding of the protein to NC to ca. 35% (Fig. 4B), while addition of LUVs to a preincubated Jbtx-FITC/NC mixture reduced the fluorescence intensity by only 25%. This suggests that changes in the structure of Jbtx and/or by sequestration of this polypeptide from solution occur upon addition of LUVs.

3.4. *Interaction of Jbtx with Bicelles*

Bicelles are currently considered the best model to study protein-membrane interactions [23,24,32]. Compared to the CD spectrum of free Jbtx, which showed a pronounced negative peak around 200 nm typical of random coil structures, the CD spectrum of Jbtx in the presence of negatively charged bicelles shows a reduced intensity in the random coil region, indicative of an increase in the polypeptide secondary structure content (Fig. 7A). In the presence of neutral bicelles, the differences in the CD spectrum are less noticeable (Fig. 7C). Superimposition of the NMR spectra of Jbtx in the absence and presence of bicelles revealed some changes in the chemical shift of a number of amino acids, even though the characteristic profile of an intrinsically disordered protein was maintained (Fig. 7B and D). The corresponding NMR spectra were similar in the two cases of neutral or negatively charged bicelles, with changes in secondary structure of Jbtx resulting more intense in the latter case (Fig. 7A and C). The analysis of the chemical shift perturbations along the peptide chain of Jbtx showed consistent changes localised at the N- and C-termini of the protein (Fig. 7E). The regions in the amino acid sequence of Jbtx that show more significant perturbations of chemical shifts in the presence of bicelles are shown in Fig. 7F.

3.4.1. *In vitro interaction of Jbtx-FITC with insect nerve cord in the presence of bicelles*

The experiments with Jbtx and insect NC in presence of negatively charged bicelles (Fig. 4C) gave results similar to those obtained for LUVs. As shown in Fig. 4C, the interaction between Jbtx-FITC and NC was decreased to about 60% after addition of bicelles prepared with 10 or 150 mM lipids. On the other hand,

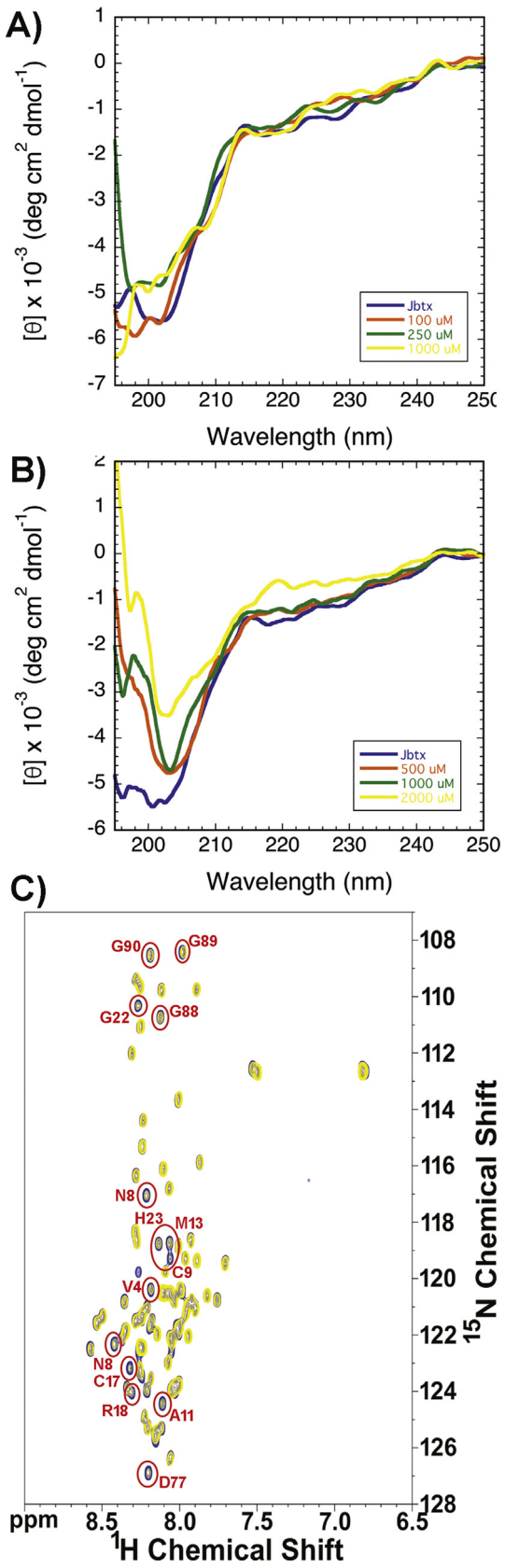

Fig. 5. Structural analysis of Jbtx in the presence of negatively charged LUVs. **A**) Circular dichroism spectrum in the presence of LUVs made using 50:50 (w/w) PC:PG. Blue, orange, green and yellow traces refer to Jbtx in the presence 0, 100, 250, and 1000 μM PC:PG LUVs, respectively. **B**) Circular dichroism spectrum of Jbtx in the presence of PG-LUVs. Blue, orange, green and yellow traces refer to Jbtx in the presence of 0, 500, 1000, and 2000 μM PG-LUVs, respectively. **C**) 700 MHz ^{1}H,^{15}N-HSQC spectra of Jbtx in the absence (blue) or presence (yellow) of 2 mM PG LUVs. Red circles highlight the amino acids with lower signal intensity in the NMR spectrum for Jbtx in the presence of PG LUVs. (For interpretation of the references to colour in this figure legend, the reader is referred to the web version of this article.)

pre-incubation of Jbtx-FITC with 150 mM lipid bicelles inhibited the binding of the polypeptide to NC to ca. 30% as indicated by fluorescence microscopy (Fig. 4C). This suggests, similarly to what observed for LUVs, that Jbtx is able to interact with the lipid bilayer of bicelles.

4. Discussion

The interaction of Jbtx with membrane lipids was postulated as the mechanism underlying the protein's insecticidal or antifungal effects, either by pore formation or by alteration of cell membrane properties, or a combination of both [3]. In the present work, we provide direct demonstration of the interaction of fluorescein-labelled Jbtx with yeast (Fig. 1) and with the cockroach nervous cord (Fig. 2). Jbtx-yeast interaction was demonstrated employing fluorescence microscopy. This interaction occurred either at 4 °C (Fig. 1A) or at 28 °C (Fig. 1B,C), the former a condition that inhibits endocytosis [38], suggesting that targets of Jbtx are present on the yeast external membrane. Here we showed that fluorescein-labelled Jbtx remains attached to cellular debris after yeast cell lysis (Fig. 1B), confirming the presence of Jbtx's ligands on the cell membranes fraction.

In order to gain information on the structure of Jbtx in the polypeptide-membrane complex, circular dichroism and NMR spectroscopy were used to monitor changes in the secondary and tertiary structure of Jbtx upon interaction with artificial membrane models. This approach was chosen, instead of using yeast or insect membranes, because the viscosity, heterogeneity, and large molecular sizes of the membrane fragments obtained after cellular lysis would hamper the structural analyses by CD or NMR.

The first model employed was made of micelles composed by SDS [21,39,40]. Although SDS micelles are a poor model for biological membranes [20], Jbtx promptly interacted with these vesicles justifying further studies on this interaction. Increasing the concentration of SDS above the CMC, an incremental modification of the secondary structure of Jbtx was observed using CD and NMR spectroscopies, and a final and stable conformation was attained (Fig. 3B and C). This observation indicates that Jbtx assumes a well-defined conformation in the presence of SDS micelles. Addition of SDS micelles disrupted the polypeptide-NC interaction (Fig. 4A), an effect that could be due either to a competitive effect of the micelles sequestrating Jbtx and hindering its binding to the NC, or to the detergent effect of SDS extracting lipids from the membrane, and leading to protein denaturation. In either case, this experiment proved the existence of Jbtx-lipid interactions. SDS micelles have been classically used to mimic membranes. However, the strong curvature of these micelles, their small size, the low similarity of their composition as compared to the lipid composition of cell membranes does not make them an optimal model for protein-membrane interaction studies. Indeed, small peptides can be over-structured in the presence of detergents [20,41]. Therefore, we complemented the study of SDS micelles with the use of artificial membranes composed of phospholipids. LUVs made of different phospholipid contents produced slight changes in the protein CD spectra, likely reflecting a modification of secondary structure. Vesicles made of a negatively charged phospholipid (PG) or a zwitterionic phospholipid (POPC), lipids previously shown to somehow interact with Jbtx [12–15], had indeed the more pronounced visible effects (Figs. 4 B, 5 B and 6 B).

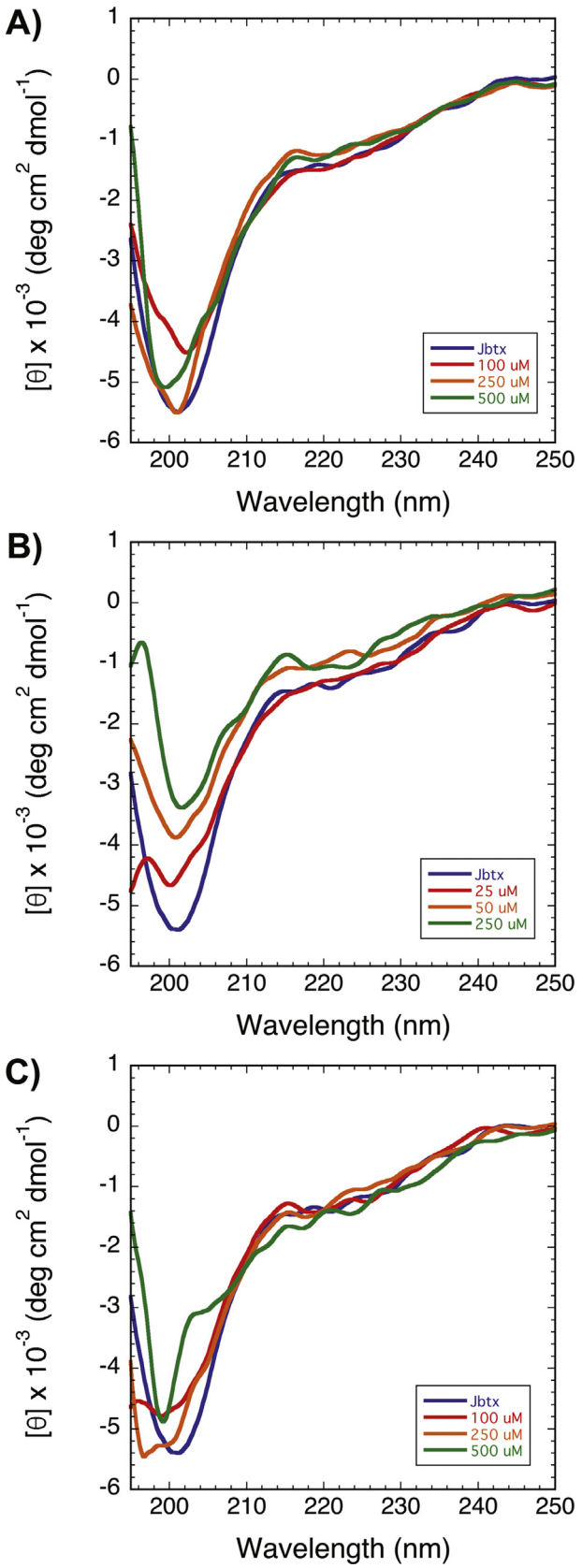

Fig. 6. Circular dichroism spectra of Jbtx in presence of LUVs of different lipids compositions. **A**) 0, 100, 250, and 500 μM PE:PC (blue, red, orange and green traces, respectively); **B**) 0, 25, 50, and 250 μM POPC (blue, red, orange and green traces, respectively); **C**) 0, 100, 250 and 500 μM 70:30 (w:w) POPC:Erg (blue, red, orange and green traces, respectively). All LUVs were prepared with buffer NaPB 50 mM at pH 6.5. (For interpretation of the references to colour in this figure legend, the reader is referred to the web version of this article.)

Jbtx binding to insect NC membranes was affected by the addition of LUVs and bicelles (Fig. 4B and C, respectively). When the polypeptide was pre-incubated with PG vesicles before addition to the NC, the fluorescence decreased to less than 50% of the initial values (Fig. 4B). A similar effect was observed when Jbtx was pre-incubated with bicelles, which caused a reduction in binding of more than 70% (Fig. 4C). This effect was seen only for Jbtx, not for bovine serum albumin, confirming the selectivity of the polypeptide interaction with lipids/phospholipids [12–15]. This result also indicated that PG vesicles competed with the insect NC membranes as a target for the binding of Jbtx. The structural changes in Jbtx seen upon its interaction with PG LUVs (Fig. 5C) were evident in the NMR analyses as decreased backbone intensity for some amino acids, consistent with a decrease in backbone mobility from a fast exchange to an intermediate exchange regime. These changes occurred in regions comprising amino acids 12–16 and 63–74, close to the N- and C-termini of the protein, previously shown by NMR to feature a transient α-helix (or single helix turn) and an α turn-like fold, respectively [5]. This observation suggests the increase of secondary structure propensity in these regions, with a local decrease of backbone mobility as compared to the peptide alone.

A third membrane model used in this study were bicelles, in which the membrane curvature further decreases as they are made of large and flat lipid bilayers. The phospholipid dimyristoylphosphatidylcholine (DMPC) organizes itself as a bilayer membrane stabilized by the addition of the detergent-like dihexanoylphosphatidylcholine (DHPC), with no aqueous portion inside the bicelle structure [24,32]. We applied CD to investigate the interaction of Jbtx with these bicelles. No significant changes in secondary structure upon exposition to electrically neutral bicelles was observed, contrasting to Jbtx's behaviour in the presence of negatively charged bicelles (Fig. 7A and C). In the latter case, the CD spectrum of Jbtx showed a decrease of ellipticity in the random coil region, likely indicating a gain of secondary structure by the protein. These changes in secondary structure did not lead to significant changes at the tertiary level, because the protein remained mostly disordered, as shown by NMR. On the other hand, either in the presence of neutral or negative bicelles, the backbone NMR chemical shifts were slightly modified, as shown in Fig. 7E. These shifts, assigned by simple inspection of the spectrum and using the criterion of signal proximity, are localised in the N- and C-terminal regions of the protein, in agreement with the modifications seen with LUVs (Fig. 5) as well as with previous results that demonstrated that these regions of Jbtx are able to cause leakage from lipid vesicles [15]. In addition, the region around residues 65–73 appears to be affected by the largest chemical shift perturbation. It is interesting to notice that this region corresponds to that for which molecular modeling studies suggested the existence of a β-hairpin motif [6,12], also observed in the crystallographic structure of JBU [44], leading to the hypothesis that it could be a factor for the membrane-disturbing activity of Jbtx [12,45]. However, later studies [14,15] appear to exclude this region as the biologically active portion of the molecule. It is possible that this region becomes important for the interaction of Jbtx with selective types of membranes.

5. ConclusionS

Using biochemical and structural approaches we investigated the structural behaviour of Jbtx in the presence of natural membranes and membrane models, showing that, when incubated with negatively charged phospholipid vesicles, the protein undergoes changes in its secondary structure and final conformation. The

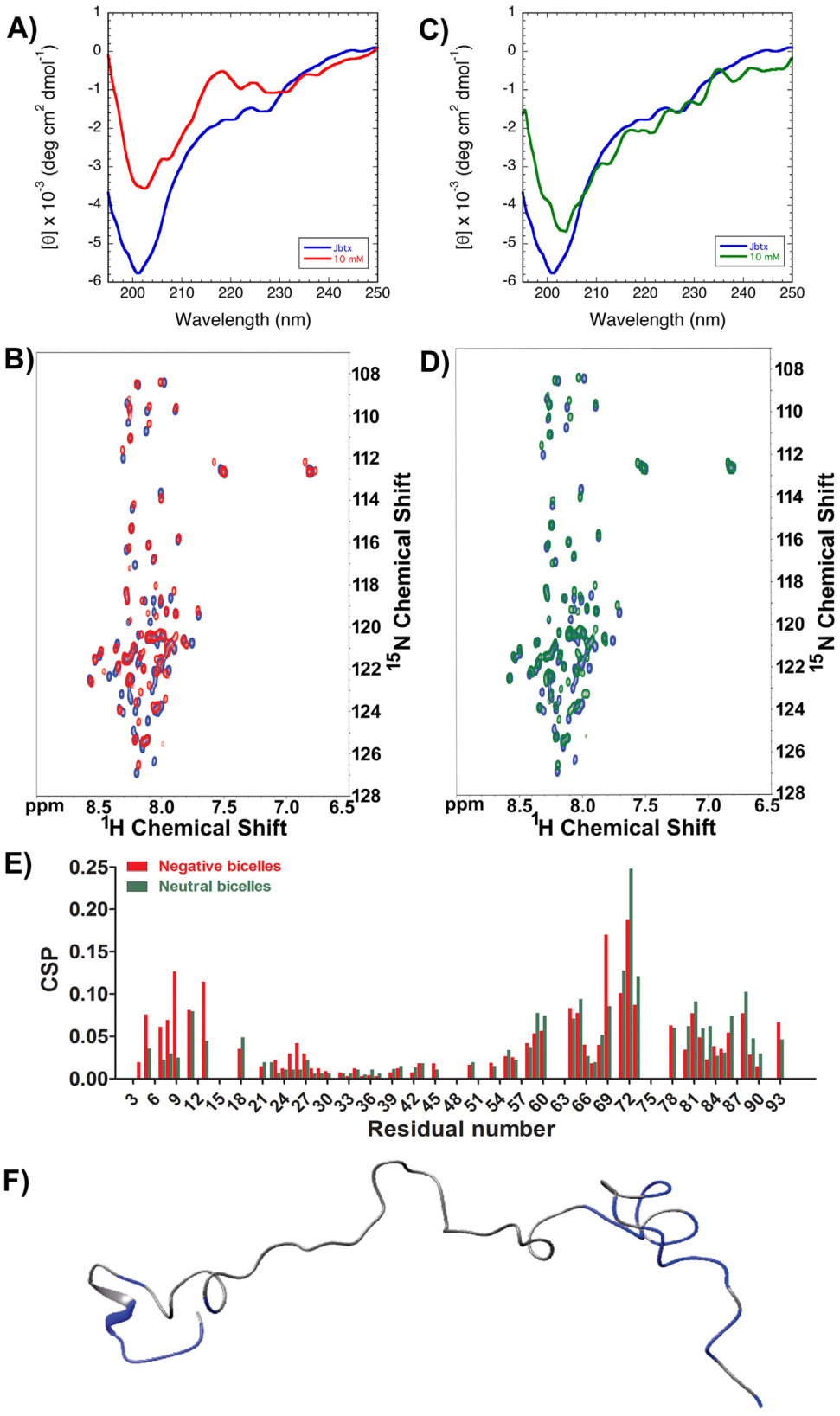

Fig. 7. Structural analysis of Jbtx in presence of bicelles. **A**) Circular dichroism spectra of Jbtx in the absence (blue) and presence (red) of 10 mM negatively charged bicelles; **B**) 700 MHz ^{1}H,^{15}N HSQC spectrum of Jbtx in the absence (blue) and presence (red) of 150 mM negatively charged bicelles; **C**) Circular dichroism spectra of Jbtx in the absence (blue) and presence (green) of 10 mM charge neutral bicelles; **D**) 700 MHz ^{1}H,^{15}N HSQC spectrum of Jbtx in the absence (blue) and presence (green) of 150 mM charge neutral bicelles; **E**) sequence-specific chemical shift perturbations (CSP) for Jbtx in presence of negatively charged (red) and charge neutral (green) bicelles. **F**) NMR structure of Jbtx (PDB code 2MM8). Amino acids highlighted in blue correspond to values of CSP > 0.025 ppm. (For interpretation of the references to colour in this figure legend, the reader is referred to the web version of this article.)

changes in the secondary structure of Jbtx in the presence of unilamellar vesicles and bicelles were less evident than in the presence of SDS micelles. An increase in the rigidity of the polypeptide backbone at its N- and C-termini segments was observed in the presence of phospholipid vesicles, and these same segments acquired secondary structure elements. Therefore, this study provides evidence supporting the hypothesis that Jbtx interacts with lipids/phospholipids, complementing previous biological assays with structural analysis of CD and NMR spectroscopic data. However, this interaction alone does not induce a complete transition of the polypeptide from an unfolded to a folded state. We speculate that Jbtx interacts with membrane phospholipids inducing small structural changes that could facilitate its binding to putative membrane receptors with acquisition of a fully folded state. Alternatively, phospholipid-bound Jbtx, although still non-structured, would insert further into the cell membrane, altering its physical properties [13] or forming ion-channel-like pores [14] that could affect cellular functions. Either or both these two mechanisms could serve as the basis for the protein toxic activities. Not all intrinsically disordered proteins become folded when meeting their binding partners. Some of them remain unfolded, even when biologically active [16,42,43]. Jbtx seems to be part of this class of IDPs, because the protein is disordered in aqueous solution and, despite its binding to lipids/phospholipids *in vivo*, it does not acquire a defined fold upon interaction with distinct types of phospholipid-based membrane models.

Author contributions

CRC and SC coordinated the project and wrote the manuscript. VB and AHSM designed the protocols, participated in all experiments and wrote the manuscript. FCL participated in the protein purification and fluorescence microscopy experiments, LLF participated in the fluorescence microscopy experiments, BZ assisted in the circular dichroism experiments, ES assisted with expression and protein purification, OD assisted with bicelles experiment design. All authors have approved the final article version.

Fundings

This work was supported by the Brazilian agency Conselho de Aperfeiçoamento de Pessoal de Nıvel Superior (CAPES), Projeto Pesquisador Visitante – PVE 054/2012, Science Without Borders and Edital Toxinologia – Nr. 63/2010; and by Conselho Nacional de Desenvolvimento Científico e Tecnológico (CNPq), Edital Universal grant 446052/2014-1. CIRMMP (Consorzio Interuniversitario di Risonanze Magnetiche di Metallo-Proteine) also supported the project by providing access to its NMR facility. VB received a split Ph.D. fellowship (PVE 054/2012) and AHSM, a Post-doctoral fellowship (BEX 8842/14-0), from CAPES, for studies at the University of Bologna, Italy.

Acknowledgments

The authors thank Massimo Lucci and Fabio Calogiuri for acquiring the NMR spectra at the Center for Magnetic Resonance (Sesto Fiorentino, Italy). The authors thank Dr. Rodrigo Ligabue-Braun for useful discussions.

Appendix A. Supplementary data

Supplementary data associated with this article can be found, in the online version, at http://dx.doi.org/10.1016/j.colsurfb.2017.08.053.

References

[1] C.R. Carlini, A.E.A. Oliveira, P. Azambuja, J. Xavier, M.A. Wells, J. Xavier-Filho, M.A. Wells, Biological effects of canatoxin in different insect models: evidence for a proteolytic activation of the toxin by insect cathepsinlike enzymes, J. Econ. Entomol. 90 (1997) 340–348, http://dx.doi.org/10.1093/jee/90.2.340.
[2] M.S. Defferrari, D.R. Demartini, T.B. Marcelino, P.M. Pinto, C.R. Carlini, Insecticidal effect of *Canavalia ensiformis* major urease on nymphs of the milkweed bug *Oncopeltus fasciatus* and characterization of digestive peptidases, Insect Biochem, Mol. Biol. 41 (2011) 388–399, http://dx.doi.org/10.1016/j.ibmb.2011.02.008.
[3] C.R. Carlini, R. Ligabue-Braun, Ureases as multifunctional toxic proteins: a review, Toxicon 110 (2016) 90–109, http://dx.doi.org/10.1016/j.toxicon.2015.11.020.
[4] C.T. Ferreira-DaSilva, M.E.C. Gombarovits, H. Masuda, C.M. Oliveira, C.R. Carlini, Proteolytic activation of canatoxin, a plant toxic protein, by insect Cathepsin-like enzymes, Arch. Insect. Biochem. Physiol. 44 (2000) 162–171, http://dx.doi.org/10.1002/1520-6327(200008)44:4<162:aid-arch3>3.0.co;2-#.
[5] F.C. Lopes, O. Dobrovolska, R. Real-Guerra, V. Broll, B. Zambelli, F. Musiani, V.N. Uversky, C.R. Carlini, S. Ciurli, Pliable natural biocide: jaburetox is an intrinsically disordered insecticidal and fungicidal polypeptide derived from jack bean urease, FEBS J. 282 (2015) 1043–1064, http://dx.doi.org/10.1111/febs.13201.
[6] F. Mulinari, F. Stanisçuaski, L.R. Bertholdo-Vargas, M. Postal, O.B. Oliveira-Neto, D.J. Rigden, M.F. Grossi-de-Sá, C.R. Carlini, Jaburetox-2Ec: an insecticidal peptide derived from an isoform of urease from the plant *Canavalia ensiformis*, Peptides 28 (2007) 2042–2050, http://dx.doi.org/10.1016/j.peptides.2007.08.009.
[7] G. Tomazetto, F. Mulinari, F. Stanisçuaski, B. Settembrini, C.R. Carlini, M. Antônio, Z. Ayub, Expression kinetics and plasmid stability of recombinant E. coli encoding urease-derived peptide with bioinsecticide activity, Enzyme Microb. Technol. 41 (2007) 821–827, http://dx.doi.org/10.1016/j.enzmictec.2007.07.006.
[8] F. Stanisçuaski, V. Te Brugge, C.R. Carlini, I. Orchard, In vitro effect of *Canavalia ensiformis* urease and the derived peptide Jaburetox-2Ec on *Rhodnius prolixus* Malpighian tubules, J. Insect Physiol. 55 (2009) 255–263, http://dx.doi.org/10.1016/j.jinsphys.2008.12.002.
[9] G.L. Galvani, L.L. Fruttero, M.F. Coronel, S. Nowicki, D.R. Demartini, M.S. Defferrari, M. Postal, L.E. Canavoso, C.R. Carlini, B.P. Settembrini, Effect of the urease-derived peptide Jaburetox on the central nervous system of *Triatoma infestans* (Insecta: heteroptera), BBA – Gen. Subj. 2015 (1850) 255–262, http://dx.doi.org/10.1016/j.bbagen.2014.11.008.
[10] L.L. Fruttero, N.R. Moyetta, A.F. Uberti, M.V. Coste Grahl, F.C. Lopes, V. Broll, D. Feder, C.R. Carlini, Humoral and cellular immune responses induced by the urease-derived peptide Jaburetox in the model organism *Rhodnius prolixus*, Parasit. Vectors. 9 (2016) 1–14, http://dx.doi.org/10.1186/s13071-016-1710-3.
[11] M. Postal, A.H.S. Martinelli, A.B. Becker-Ritt, R. Ligabue-Braun, D.R. Demartini, S.F.F. Ribeiro, G. Pasquali, V.M. Gomes, C.R. Carlini, Antifungal properties of *Canavalia ensiformis* urease and derived peptides, Peptides 38 (2012) 22–32, http://dx.doi.org/10.1016/j.peptides.2012.08.010.
[12] P.R. Barros, H. Stassen, M.S. Freitas, C.R. Carlini, M.A.C. Nascimento, C. Follmer, Membrane-disruptive properties of the bioinsecticide Jaburetox-2Ec: implications to the mechanism of the action of insecticidal peptides derived from ureases, BBA – Proteins Proteomics 2009 (1794) 1848–1854, http://dx.doi.org/10.1016/j.bbapap.2009.09.001.
[13] Y.M.S. Micheletto, C.F. Moro, F.C. Lopes, R. Ligabue-Braun, A.H.S. Martinelli, C.M. Marques, A.P. Schroder, C.R. Carlini, N.P. da Silveira, Interaction of jack bean (*Canavalia ensiformis*) urease and a derived peptide with lipid vesicles, Colloids Surf. B Biointerfaces 145 (2016) 576–585, http://dx.doi.org/10.1016/j.colsurfb.2016.05.063.
[14] A.R. Piovesan, A.H.S. Martinelli, R. Ligabue-Braun, J.-L. Schwartz, C.R. Carlini, Canavalia ensiformis *Canavalia ensiformis* urease, Jaburetox and derived peptides form ion channels in planar lipid bilayers, Arch. Biochem. Biophys. 547 (2014) 6–17, http://dx.doi.org/10.1016/j.abb.2014.02.006.
[15] A.H.S. Martinelli, K. Kappaun, R. Ligabue-Braun, M.S. Defferrari, A.R. Piovesan, F. Stanisçuaski, D.R. Demartini, C.A. Dal Belo, C.G.M. Almeida, C. Follmer, H. Verli, C.R. Carlini, G. Pasquali, Structure–function studies on jaburetox, a recombinant insecticidal peptide derived from jack bean (*Canavalia ensiformis*) urease, Biochim. Biophys. Acta – Gen. Subj. 1840 (2014) 935–944, http://dx.doi.org/10.1016/j.bbagen.2013.11.010.
[16] V.N. Uversky, Unusual biophysics of intrinsically disordered proteins, BBA – Proteins Proteomics. 1834 (2013) 932–951, http://dx.doi.org/10.1016/j.bbapap.2012.12.008.
[17] V.N. Uversky, Dancing protein clouds: the strange biology and chaotic physics of intrinsically disordered proteins, J. Biol. Chem. 291 (2016) 6681–6688, http://dx.doi.org/10.1074/jbc.R115.685859.
[18] P. Tompa, M. Fuxreiter, Fuzzy complexes: polymorphism and structural disorder in protein–protein interactions, Trends Biochem. Sci. 33 (2008) 2–8, http://dx.doi.org/10.1016/j.tibs.2007.10.003.
[19] V.N. Uversky, Intrinsically disordered proteins and their environment: effects of strong denaturants, temperature, pH, counter ions, membranes, binding partners, osmolytes, and macromolecular crowding, Protein J. 28 (2009) 305–325, http://dx.doi.org/10.1007/s10930-009-9201-4.

[20] L. Mäler, Solution NMR studies of cell-penetrating peptides in model membrane systems, Adv. Drug Deliv. Rev. 65 (2013) 1002–1011, http://dx.doi.org/10.1016/j.addr.2012.10.011.
[21] D. Otzen, Protein–surfactant interactions: a tale of many states, BBA – Proteins Proteomics 1814 (2011) 562–591, http://dx.doi.org/10.1016/j.bbapap.2011.03.003.
[22] M. Baginski, B. Cybulska, W.I. Gruszecki, Chapter 9 – Interaction of polyene macrolide antibiotics with lipid model membranes, Adv. Planar Lipid Bilayers Liposomes 3 (2006) 269–329, http://dx.doi.org/10.1016/S1554-4516(05)03009-7.
[23] C.R. Sanders, R.S. Prosser, Bicelles: a model membrane system for all seasons? Structure 6 (1998) 1227–1234, http://dx.doi.org/10.1016/S0969-2126(98)00123-3.
[24] A. Diller, C. Loudet, F. Aussenac, G. Raffard, S. Fournier, M. Laguerre, A. Grélard, S.J. Opella, F.M. Marassi, E.J. Dufourc, Bicelles A natural molecular goniometer for structural, dynamical and topological studies of molecules in membranes, Biochimie 91 (2009) 744–751, http://dx.doi.org/10.1016/j.biochi.2009.02.003.
[25] C. Loudet, A. Diller, A. Grélard, R. Oda, E.J. Dufourc, Biphenyl phosphatidylcholine: a promoter of liposome deformation and bicelle collective orientation by magnetic fields, Prog. Lipid Res. 49 (2010) 289–297, http://dx.doi.org/10.1016/j.plipres.2010.02.002.
[26] J.A. Whiles, K.J. Glover, R.R. Vold, E.A. Komives, Methods for studying transmembrane peptides in bicelles: consequences of hydrophobic mismatch and peptide sequence, J. Magn. Reson. 158 (2002) 149–156, http://dx.doi.org/10.1016/S1090-7807(02)00068-X.
[27] M. Bradford, A rapid and sensitive method for the quantification of microgram quantities of protein utilizing the principle of protein-dye binding, Anal. Biochem. 72 (1976) 248–254, http://dx.doi.org/10.1016/0003-2697(76)90527-3.
[28] J.A. Glasel, Validity of nucleic acid purities monitored by 260 nm/280 nm absorbance ratios, Biotechniques 18 (1995) 62–63 http://www.ncbi.nlm.nih.gov/pubmed/7702855.
[29] T.S. Banipal, H. Kaur, P.K. Banipal, A.K. Sood, Effect of head groups, temperature, and polymer concentration on surfactant – Polymer interactions, J. Surfactants Deterg. 17 (2014) 1181–1191, http://dx.doi.org/10.1007/s11743-014-1633-y.
[30] M. Hope, M. Bally, G. Webb, P. Cullis, Production of large unilamellar vesicles by a rapid extrusion procedure. Characterization of size distribution, trapped volume and ability to maintain a membrane potential, Biochim. Biophys. Acta. 812 (1985) 55–65, http://dx.doi.org/10.1016/0005-2736(85)90521-8.
[31] B. Mui, L. Chow, M.J. Hope, Extrusion technique to generate liposomes of defined size, Methods Enzymol. 367 (2003) 3–14, http://dx.doi.org/10.1016/S0076-6879(03)67001-1.
[32] M. Beaugrand, A.A. Arnold, J. Me Hein, D.E. Warschawski, P.T.F. Williamson, I. Marcotte, Lipid concentration and molar ratio boundaries for the use of isotropic bicelles, Langmuir ACS J. Surfaces Colloids. 30 (2014) 6162–6170, http://dx.doi.org/10.1021/la5004353.
[33] L. Mäler, A. Gräslund, Artificial membrane models for the study of macromolecular delivery, Methods Mol. Biol. 480 (2009) 129–139, http://dx.doi.org/10.1007/978-1-59745-429-2_9.
[34] G.T. Hermanson, Bioconjugate Techniques, Academic Press, 1996.
[35] F. Sherman, Getting started with yeast, Methods Enzymol. 350 (2002) 3–41, http://dx.doi.org/10.1016/S0261-3069(97)88930-3.
[36] C.A. Rohl, R.L. Baldwin, Articles comparison of NH exchange and circular dichroism as Techniques for measuring the parameters of the helix-coil transition in peptidest, Bai Englander. 36 (1972) 8435–8442, http://dx.doi.org/10.1021/bi9706677.
[37] E. Baraldi, E. Coller, L. Zoli, A. Cestaro, S.C.E. Tosatto, B. Zambelli, Unfoldome variation upon plant-pathogen interactions: strawberry infection by *Colletotrichum acutatum*, Plant Mol. Biol. (2015), http://dx.doi.org/10.1007/s11103-015-0353-7.
[38] R.E. Pagano, L. Huang, C. Wey, Interaction of phospholipid vesicles with cultured mammalian cells, Nature 252 (1974) 166–167, http://dx.doi.org/10.1038/252166a0.
[39] R.M. Garavito, S. Ferguson-Miller, Detergents as tools in membrane biochemistry, J. Biol. Chem. 276 (2001) 32403–32406, http://dx.doi.org/10.1074/jbc.R100031200.
[40] V. Opatova, M.A. Arnedo, Spiders on a hot volcanic roof: colonisation pathways and phylogeography of the canary islands endemic trap-door spider *Titanidiops canariensis* (araneae, idiopidae), PLoS One 9 (2014), http://dx.doi.org/10.1371/journal.
[41] P. Damberg, J. Jarvet, A.J. Gräslund, Micellar systems as solvents in peptide and protein structure determination, Methods Enzymol. 339 (2001) 271–285, http://dx.doi.org/10.1016/S0076-6879(01)39318-7.
[42] V.N. Uversky, The multifaceted roles of intrinsic disorder in protein complexes, FEBS Lett. 589 (2015) 2498–2506, http://dx.doi.org/10.1016/j.febslet.2015.06.004.
[43] E. Hazy, P. Tompa, Limitations of induced folding in molecular recognition by intrinsically disordered proteins, Chemphyschem 10 (2009) 1415–1419, http://dx.doi.org/10.1002/cphc.200900205.
[44] A. Balasubramanian, K. Ponnuraj, Crystal structure of the first plant urease from jack bean: 83 years of journey from its first crystal to molecular structure, J. Mol. Biol. 400 (2010) 274–283, http://dx.doi.org/10.1016/j.jmb.2010.05.009.
[45] A. Balasubramanian, N. Balaji, N. Gautham, K. Ponnuraj, Molecular dynamics simulation and molecular modelling studies on the insecticidal domain from jack bean urease, J. Mol. Biol. 39 (2013) 357–366, http://dx.doi.org/10.1080/08927022.2012.729271.